Dynamics-Induced Surface Metallization of Si(100)

Luca Gavioli, Maria Grazia Betti, and Carlo Mariani
Istituto Nazionale per la Fisica della Materia, Dipartimento di Fisica, Università di Modena, via G. Campi 213/A, I-41100 Modena, Italy
(Received 21 June 1996)

High-temperature surface metallization of Si(100) is observed at $T > 900$ K by high-resolution electron-energy-loss and ultraviolet photoemission spectroscopy. Metallization takes place well below the incomplete surface melting temperature and is consistent with the Si dimer dynamics, characterized by an *instantaneous symmetriclike dimer* configuration. The surface free carrier concentration in the metallic phase has been evaluated, reaching (at 1170 K) the same order of magnitude of the surface dimer density. [S0031-9007(96)01536-0]

PACS numbers: 71.20.Mq, 73.20.Mf, 73.61.Cw

The basic feature of reconstructed Si(100) surface is the presence of Si-Si dimers, formed by bonding of the two topmost layer Si atoms. This surface symmetry is consistent with both symmetric (SD) and asymmetric (AD) dimer disposition [1], though it has been recently established that the AD configuration is the reconstruction [2–7] consistent with the semiconducting character of the surface [8]. At very low temperature large regions of AD present a $c(4 \times 2)$ symmetry [2–4,9,10], energetically degenerate with a $p(2 \times 2)$ reconstruction [11–13]. The surface dynamics (AD flip-flop and twist motion [13]) determines an order-disorder transition observed around 200 K [2,3,12,14], leading to the room-temperature–(2×1) surface symmetry. This ordered dimer structure persists even at high temperatures (1200 K) [15,16], while the surface undergoes an incomplete melting transition at $T_{\text{im}} \sim 1400$ K, characterized by the formation of a liquid layer in the two topmost surface planes [17]. The semiconducting nature of this surface, established by several electron spectroscopies [18–26], has been associated with dimer-related surface electronic states. A question arises as to how the AD dynamics as a function of temperature is accompanied by modifications in the surface electronic structure and whether a semiconductor-metal transition is induced by the surface dynamics or by the incomplete surface melting.

In this Letter we present experimental evidence of high temperature *surface metallization* more than 300 K *below the incomplete melting transition* temperature T_{im}, obtained with high-resolution electron-energy-loss spectroscopy (HREELS) and ultraviolet-photoemission spectroscopy (UPS). We attribute the Si(100) surface metallization mainly to the *surface dimer dynamics*; i.e., the increased dimer flipping rate at finite temperature leads to a fast time alternation of the local $c(4 \times 2)$ and $p(2 \times 2)$ stable phases, passing through nearly symmetric flat dimer configurations [13]. Upon raising the temperature, well below T_{im}, the influence of this instantaneous dimer-induced symmetric geometry is expected to deeply affect the electronic properties, leading to high density of free carriers at the surface.

Ultraviolet photoemission spectroscopy can directly give information on surface metallization by enlightening the occupied electronic states up to the Fermi level. Low-energy inelastic electron scattering (HREELS) is particularly sensitive to the surface conductivity through analysis of free-carrier induced collective modes [27–29]. Thus, these complementary spectroscopies are among the most suitable techniques to exploit insulator-metal transitions at semiconductor surfaces.

The experiment was performed on n-type doped Si(100) wafer with $n \approx 1 \times 10^{19}$ cm^{-3} donor (Sb) concentration. The surface was prepared with appropriate etching procedure [30], fast entry into ultrahigh vacuum (UHV, base pressure in the 10^{-11} mbar range), subsequent annealing at 850 K for several hours, and flash at 1200 K for 1 min. Cleanness was checked with HREELS and Auger spectroscopy. The sample was directly Ohmically heated by a current pulsed at a few Hz, suspending the data acquisition when the current was on. The temperature was measured with a thermocouple placed on the sample holder very close to the wafer surface and with infrared pyrometers. Thanks to the high dopant concentration, the temperature was quite uniform over the whole surface. The HREELS spectra were taken in the specular geometry with a primary beam energy $E_p = 7.8$ eV and an angle of 62.5°. Sampling depth was of the order of a few tens of Å, estimated considering the electron inelastic scattering process [29]. The UPS data were collected using 21.2 eV He I photons with a double-pass cylindrical mirror electron analyzer (CMA) integrating over different emission angles. The sampling depth, estimated by the electron mean free path at ~17 eV kinetic energy, was about 6 Å [31]. At room temperature (RT) the low-energy electron diffraction (LEED) presents a sharp (2×1) double-domain diffraction pattern, which is still visible at $T \sim 1050$ K with broad spots, in agreement with the scanning tunneling microscopy (STM) observation of dimer structure at this temperature [15].

The HREELS data in the quasielastic peak energy region as a function of surface temperature are shown in Fig. 1. The main effect of temperature raising is a distinct

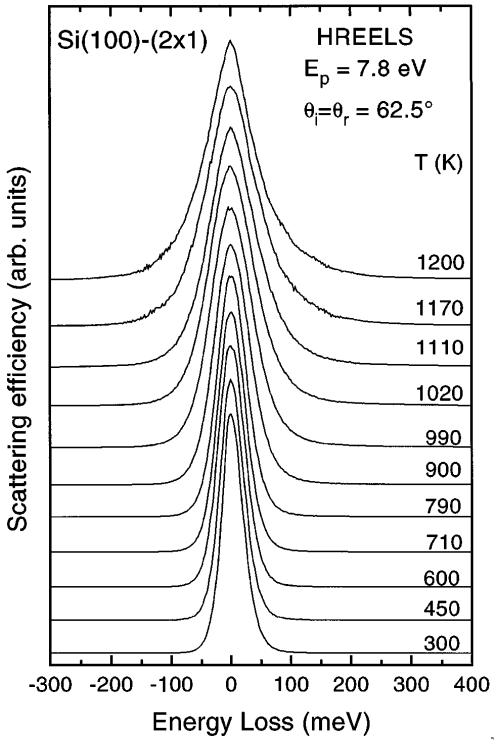

FIG. 1. High-resolution electron-energy-loss spectroscopy data in the quasielastic peak energy region, as a function of the surface temperature. Primary beam energy $E_p = 7.8$ eV, incidence (ϑ_i) and collecting (ϑ_r) angles of 62.5°. Spectra are stacked along the vertical axis for clarity.

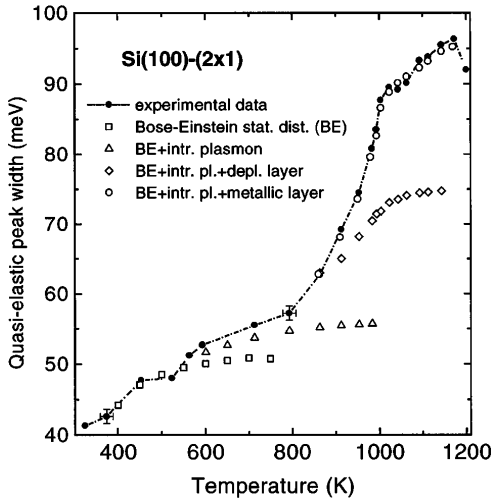

FIG. 2. Quasielastic peak width as a function of temperature. Experimental data (dash-dotted black line). Results of the dielectric model calculations including: Bose-Einstein (BE) statistical distribution thermal variation (open squares); BE + intrinsic carrier plasmon thermal variations (open triangles); BE + intrinsic carrier + depletion layer thickness thermal variations (open diamonds); BE + intrinsic plasmon + topmost metallic layer plasmon variations (open dots).

widening of the quasielastic peak. Its corresponding full-width at half-maximum (FWHM) behavior is plotted in Fig. 2, where three different phases can be easily distinguished. As the temperature is raised from 300 to 600 K, we observe a slight peak widening, due to the multiple excitation of surface plasmons associated with the thermally excited dopant-induced free carriers in the bulk. The second phase, starting around 800 K, is characterized by a huge quasielastic peak width increase, not accounted for by simple free-carriers thermal excitation mechanism. A further variation in the linewidth broadening rate determines the onset of the third phase, covering the 1000–1200 K temperature range, ending up with a saturation followed by a small decrease.

Quantitative evaluation of the energy-loss spectrum can be performed using a simple dielectric model [27–29]. In the dipole scattering approximation, the scattering efficiency is proportional to the electron inelastic scattering probability $P(q, \omega)$, which can be expressed as the product of three terms: a "kinematic factor" (containing the geometry of the process), the Bose-Einstein statistical distribution factor (containing the temperature dependent states occupancy), and the loss function $f(q, \omega) = -\mathrm{Im}\{1/[1 + \varepsilon_{\mathrm{eff}}(q, \omega)]\}$ (containing the physical response), where $\varepsilon_{\mathrm{eff}}(q, \omega)$ is the effective dielectric function (DF) of the medium. We assume that the physical system is constituted by different layers, namely, the semi-infinite Si bulk and a surface layer, which can be depleted of dopant-induced free carriers (so-called dead or depletion layer [32]). Each layer is characterized by its DF. In this energy region, the bulk is described by the infrared infinite dielectric constant (ε_∞) and by a uniform dopant-induced free-carrier electron plasmon, with a plasmon energy $\omega_p = \sqrt{4\pi n e^2/m^*}$ (with n the free-carrier density, e the electron charge, and m^* the optical effective mass in the Si conduction band). The dead layer region is depleted of free carriers, thus the plasmon excitation is absent.

The experimental scattering efficiency is fitted by using the dielectric model [33], obtaining the experimental quasielastic peak line shape and the low energy-loss region as a function of temperature. Choosing the appropriate values for m^* ($0.26 \times m_0$, with m_0 the free electron mass) [34] and relaxation time $\tau(1.4 \times 10^{-14}$ s) [35] corresponding to the actual doping level ($n \sim 10^{19}$ electrons/cm^3), we calculate a bulk dopant-induced plasmon frequency $\omega_p = 230$ meV (corresponding surface plasmon at 64 meV) with a damping of 280 meV, consistent with the absence of distinct low-frequency peaks in the spectra (see Fig. 1). Using this simplified model with a semi-infinite bulk and a depletion layer thickness of 45 Å [36], we obtain a good fit to the experimental data at RT.

Keeping the temperature as the only variable fitting parameter, the experimental linewidth broadening plotted in Fig. 2 can be accounted for only in the first phase (300–600 K): thus, in the temperature range the linewidth increase is only due to the Bose-Einstein statistical distribution factor (white squares in Fig. 2). Above 600 K, some other mechanism must contribute to the linewidth

broadening. Inclusion of thermal activation of intrinsic conduction carriers across the Si energy gap in the model (triangles in Fig. 2) improves the curve, but is not sufficient to fit the huge quasielastic peak broadening above 800 K. Decrease of the depletion layer thickness has been invoked to explain high-temperature quasielastic peak widening at the Si(111)-(7 × 7) surface [37]. The depletion layer thickness was included as a fitting parameter and by decreasing its thickness we were able to obtain a result more consistent with the experiment (open diamonds in Fig. 2); however, this model fails above 840 K. Beyond this temperature, only inclusion of a topmost thin *metallic* layer can account for the experimental linewidth broadening (open dots in Fig. 2). We introduce in the dielectric model a slab characterized by a Drude-like free-electron gas, described by an effective dielectric function

$$\varepsilon_s(\omega) = \varepsilon_\infty - \left(\frac{\omega_p}{\omega}\right)^2 \frac{1}{1 - 1/i\omega\tau},$$

with a thickness of 1.7 Å (equivalent to the topmost Si dimer layer). Using this model a very good agreement with the experiment was obtained by raising the free-electron plasmon frequency from ~0.6 to 4.3 eV (with 1.7 eV damping), upon increasing the temperature from 850 to 1170 K. The plasmon frequency values correspond to a *metallic* layer with an "equivalent" surface free-carrier concentration raising from 0.4×10^{13} electrons/cm^{-2} to 2.2×10^{14} electrons/cm^{-2}, as a function of temperature. The last fit value is comparable to the surface dimer density (6.8×10^{14} cm^{-2}), thus indicating an actual *surface metallic* behavior. Finally, we notice that at the highest temperature reached in the HREELS experiment (1200 K), there is a slight linewidth narrowing, which can be presumably related to a larger metallic screening of the underlying bulk collective modes.

The presence of a surface metallic character is even more evident from Fig. 3, where UPS data in the valence band (VB) region are plotted as a function of surface temperature. At room temperature, the density of states (DOS) is characterized by the filled dangling-bond surface states at about 0.8 eV binding energy and by further higher-energy structures, in agreement with previous measurements [18–21]. Upon increasing temperature, the main DOS features clearly broaden but do not appreciably change till 900 K. At about 1000 K and even more at 1200 K, the main VB structures are deeply modified; in particular, a finite and distinct nonzero DOS is present at the Fermi level, indicating *surface metallization*. This evidence is consistent with the HREELS observations at the same temperature. Metallization occurs at the surface, since the bulk is semiconducting at these temperatures. The DOS assumes a definite metalliclike Fermi edge shape in the 1200–1350 K temperature range, still a few tens of K below the Si(100) incomplete melting temperature (1400 K) [17]. We briefly point out that incomplete surface melting differs from proper surface melting [38] in that the thickness of the molten surface layer does uniformly increase

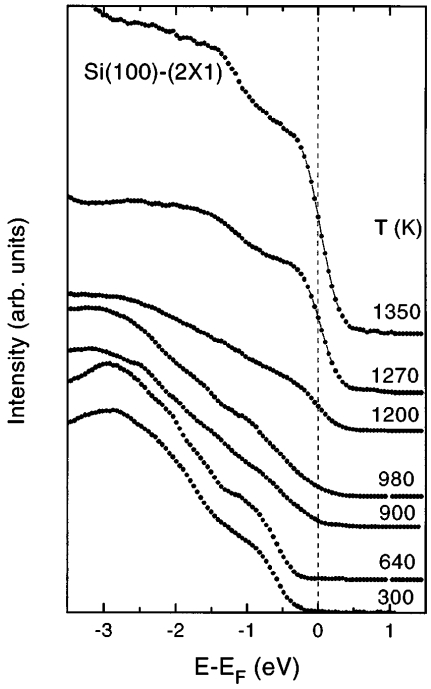

FIG. 3. Valence band ultraviolet (He I photon energy, 21.2 eV) angle-integrated photoemission data, as a function of the surface temperature. The Fermi level position (measured on clean metallic Mo in electrical contact with the Si sample) is indicated with a vertical dashed line.

with temperature, but remains constant in a wide temperature range. This effect has been predicted for face centered cubic crystals on the basis of thermodynamical and molecular-dynamics calculations [39]. Among semiconductors, it has been theoretically predicted [40] and experimentally observed [41–43] at the Ge(111) surface.

What is the origin of this *metallic* behavior of the topmost Si surface layer at relatively low temperatures ($T \ll T_{\text{im}}$)? In our opinion surface metallization is to be attributed to the flipping and twisting motion of the Si dimers [13], to electron-phonon interaction and to the possible partial breaking/rebuilding of dimer bonds (at higher temperatures). The dimer flip-flop motion is present even at room temperature [13], but above 800 K its frequency is so high that the average time spent by the dimers in a flat *instantaneous symmetriclike configuration* strongly affects the surface electronic structure. In fact, the unoccupied electronic states associated with the AD geometry move to lower energy when considering the symmetric dimers geometry [1,44], giving rise to a surface state crossing the Fermi level in a wide range of the surface Brillouin zone, forming a metallic surface. Thus, considering the dimers dynamics, the observed first layer metallization can be mainly ascribed to the time-averaged geometry assumed by the dimers during the flip-flop and twist motion. At higher temperatures (above 1200 K) a possible contribution to the metallic-shaped Fermi edge could also come from partial breaking/reforming of the flipping dimers, leaving two partially occupied dangling bonds per atom (as in the ideal truncated surface) [1].

Nevertheless, the presence of dimers and steps on the Si(100) surface even above 1400 K [16], suggests a minor contribution of this mechanism to the metallization.

It is worth noting the peculiar behavior of the Si(100) surface, due to the dimer dynamics. The dimer flip-flop and twist motion characterizes the electronic and structural properties of this surface from very low temperatures (80 K) to the incomplete melting transition (1400 K), inducing a series of structural and electronic phase transitions: (i) an order-disorder phase transition at $\sim$200 K, where the surface moves from the local $c(4 \times 2)$ and $p(2 \times 2)$ symmetries to a nominal (2×1) reconstruction, also modifying the occupied and unoccupied surface electronic states [20]; (ii) the semiconductor-metal transition above 1000 K, where the instantaneous symmetriclike flat dimer geometry dominates the surface dielectric response; (iii) the incomplete melting transition at 1400 K with the formation of a molten interface between the crystalline bulk and vacuum.

In summary, we have shown that the clean Si(100) surface undergoes a semiconductor-metal transition above 900 K, well below the incomplete surface melting temperature. The metallization, estimated to correspond to a free carrier density equivalent to about $1/3$ of the surface dimer density, at 1170 K, is due to the temperature-induced instantaneous symmetriclike configuration of the surface Si dimers dynamics.

We thank Silvio Modesti for fruitful discussion, Carlo Maria Bertoni for a critical reading of the manuscript, and Paola Petroni for helpful linguistic assistance. This work was partially supported by INFM under advanced research project "LOTUS."

[1] D. J. Chadi, Phys. Rev. Lett. **43**, 43 (1979).
[2] T. Tabata, T. Aruga, and Y. Murata, Surf. Sci. Lett. **179**, L63 (1987).
[3] K. Kubota and Y. Murata, Phys. Rev. B **49**, 4810 (1994).
[4] R. A. Wolkow, Phys. Rev. Lett. **68**, 2636 (1992).
[5] N. Jedrecy, M. Sauvage-Simkin, R. Pinchaux, J. Massies, N. Greiser, and V. H. Etgens, Surf. Sci. **230**, 197 (1990).
[6] A. I. Shkrebtii and R. Del Sole, Phys. Rev. Lett. **70**, 2645 (1993).
[7] P. Krüger and J. Pollmann, Phys. Rev. Lett. **74**, 1155 (1995).
[8] F. J. Himpsel and D. E. Eastman, J. Vac. Sci. Technol. **16**, 1297 (1979).
[9] D. Badt, H. Wegenlnik, and H. Neddermeyer, J. Vac. Sci. Technol. B **12**, 2015 (1994).
[10] H. Tochihara, T. Amakusa, and M. Iwatsuki, Phys. Rev. B **50**, 12 262 (1994).
[11] Z. Zhu, N. Shima, and M. Tukada, Phys. Rev. B **40**, 11 868 (1989).
[12] K. C. Low and C. K. Ong, Phys. Rev. B **50**, 5352 (1994).
[13] A. I. Shkrebtii, R. Di Felice, C. M. Bertoni, and R. Del Sole, Phys. Rev. B **51**, 11 201 (1995).
[14] K. Inoue, Y. Morikawa, K. Terakura, and M. Nakayama, Phys. Rev. B **49**, 14 774 (1994).
[15] H. Tokumoto and M. Iwatsuki, Jpn. J. Appl. Phys. **32**, 1368 (1993).
[16] J. J. Metois and D. E. Wolf, Surf. Sci. **298**, 71 (1993).
[17] J. Fraxedas, S. Ferrer, and F. Comin, Europhys. Lett. **25**, 119 (1994).
[18] P. Mårtensson, A. Cricenti, and G. V. Hansson, Phys. Rev. B **33**, 8855 (1986).
[19] R. D. Bringans, R. I. G. Uhrberg, M. A. Olmstead, and R. Z. Bachrach, Phys. Rev. B **34**, 7447 (1986).
[20] Y. Enta, S. Suzuki, and S. Kono, Phys. Rev. Lett. **65**, 2704 (1990).
[21] A. Cricenti, D. Purdie, and B. Reihl, Surf. Sci. **331–333**, 1033 (1995).
[22] R. J. Hamers, R. M. Tromp, and J. E. Demuth, Surf. Sci. **181**, 346 (1987).
[23] A. W. Munz, Ch. Ziegler, and W. Göpel, Phys. Rev. Lett. **74**, 2244 (1995).
[24] Y. J. Chabal, S. B. Christman, E. E. Chaban, and M. T. Yin, J. Vac. Sci. Technol. A **1**, 1241 (1983).
[25] H. H. Farrel, F. Stucki, J. Anderson, D. J. Frankel, G. J. Lapeyre, and M. Levinson, Phys. Rev. B **30**, 721 (1984).
[26] L. Gavioli, M. G. Betti, A. Cricenti, and C. Mariani, J. Electron Spectrosc. Relat. Phenom. **76**, 541 (1995).
[27] B. N. J. Persson and J. E. Demuth, Phys. Rev. B **30**, 5968 (1994).
[28] D. L. Mills, Surf. Sci. **48**, 59 (1975).
[29] H. Ibach and D. L. Mills, *Electron Energy Loss Spectroscopy and Surface Vibrations* (Academic Press, New York, 1982).
[30] A. Ishizaka and Y. Shiraki, J. Electrochem. Soc. **133**, 666 (1986).
[31] M. P. Seah and W. A. Dench, Surf. Interface Anal. **1**, 2 (1979).
[32] S. R. Streight and D. L. Mills, Phys. Rev. B **40**, 10 488 (1989), and references therein.
[33] Ph. Lambin, J. P. Vigneron, and A. A. Lucas, Phys. Rev. B **32**, 8203 (1985); Ph. Lambin, J. P. Vigneron, A. A. Lucas, Comput. Phys. Commun. **60**, 351 (1990).
[34] C. Jacoboni and L. Reggiani, Adv. Phys. **28**, 493 (1979).
[35] *Numerical Data and Functional Relationships in Science and Technology*, Landolt-Börnstein, Group III, Vol. 17a (Springer-Verlag, Berlin, 1982).
[36] S. M. Sze, *Physics of Semiconductor Devices* (Wiley-Interscience, New York, 1969).
[37] J. A. Stroscio and W. Ho, Phys. Rev. Lett. **54**, 1573 (1985).
[38] M. Bienfait, Surf. Sci. **272**, 1 (1992).
[39] A. Trayanov and E. Tosatti, Phys. Rev. Lett. **59**, 2207 (1987); P. Carnevali, F. Ercolessi, and E. Tosatti, Phys. Rev. B **36**, 6701 (1987).
[40] N. Takeuchi, A. Selloni, and E. Tosatti, Phys. Rev. Lett. **72**, 2227 (1994).
[41] A. W. Denier van der Gon, J. M. Gay, J. W. M. Frenken, and J. F. van der Veen, Surf. Sci. **241**, 335 (1991).
[42] T. T. Tran, S. Thevuthasan, Y. J. Kim, D. J. Friedman, A. P. Kaduwela, G. S. Herman, and C. S. Fadley, Surf. Sci. **281**, 270 (1993).
[43] S. Modesti, V. R. Dhanak, M. Sancrotti, A. Santoni, B. N. J. Persson, and E. Tosatti, Phys. Rev. Lett. **73**, 1951 (1994).
[44] M. Rholfing, P. Kruger, and J. Pollmann, Phys. Rev. B **52**, 13 753 (1995).